10 Interdiffusion and Kirkendall Effect

Diffusion processes in alloys with composition gradients are of great practical interest. In the preceding chapters, we have assumed that the concentration gradient is the only cause for flow of matter. Such situations can be studied using small amounts of trace elements in otherwise homogeneous materials. We will discuss the experimental procedure for tracer experiments in Chap. 13. From a general viewpoint, the diffusion flux is proportional to the gradient of the *chemical potential*. The chemical potential is proportional to the concentration gradient only for dilute systems or ideal solid solutions. The gradient of the chemical potential gives rise to an 'internal' driving force and the intermixing of a binary A-B system can be described by a concentration-dependent *chemical* or *interdiffusion coefficient*. In a binary alloy there is a single interdiffusion coefficient that characterises interdiffusion. The interdiffusion coefficient is usually a composition-dependent quantity. On the other hand, interdiffusion is due to the diffusive motion of A and B atoms, which in general have different *intrinsic diffusion coefficients*. This difference manifests itself in the *Kirkendall effect*, a shift of the diffusion zone with respect to the ends of the diffusion couple. We consider first interdiffusion and the Boltzmann-Matano and Sauer-Freise methods for the determination of the interdiffusion coefficient. Further sections are devoted to intrinsic diffusion, Kirkendall effect, and to the Darken relations. The Darken-Manning relations, the so-called vacancy-wind effect, and the stability or instability of Kirkendall planes are described. A discussion of interdiffusion in ionic systems and the Nernst-Planck equation and its relation to the Darken equation is postponed to the end of the next chapter.

10.1 Interdiffusion

Let us consider a binary diffusion couple, in which the chemical composition varies in the diffusion zone over a certain range. Diffusing atoms then experience different chemical environments and hence have different diffusion coefficients. As already mentioned in Chap. 2, this situation is called *interdiffusion* or *chemical diffusion*. We use the symbol $\tilde{D}$ to indicate that

the diffusion coefficient is concentration-dependent and call it the *interdiffusion or chemical diffusion coefficient*. Fick's second law Eq. (2.5) then reads

$$\frac{\partial C}{\partial t} = \frac{\partial}{\partial x}\left[\tilde{D}(C)\frac{\partial C}{\partial x}\right] = \tilde{D}(C)\frac{\partial^2 C}{\partial x^2} + \frac{\mathrm{d}\tilde{D}(C)}{\mathrm{d}C}\left(\frac{\partial C}{\partial x}\right)^2 . \tag{10.1}$$

The second term on the right-hand side represents an *'internal driving force'* (see also Chap. 11). Mathematically, Eq. (10.1) is a non-linear partial differential equation. For an arbitrary concentration dependence of $\tilde{D}(C)$ it can usually be not solved analytically. In addition, theoretical models which permit the calculation of the composition-dependent diffusivity from deeper principles are at present not broadly available.

The strategy illustrated in Chaps. 2 and 3 for calculating the concentration field for given initial and boundary conditions is not applicable to interdiffusion. We shall see, however, that it is possible to determine the concentration-dependent diffusivity, $\tilde{D}$, from a measured concentration field by using Eq. (10.1). Two methods for extracting diffusivities from concentration-depth profiles – the classical *Boltzmann-Matano method* and related approaches proposed by *Sauer and Freise* – are considered below. Boltzmann's transformation of Fick's second law is fundamental for both methods and is discussed first.

10.1.1 Boltzmann Transformation

In 1894 the famous Ludwig Boltzmann [1] showed that the nonlinear partial differential equation (10.1) can be transformed to a nonlinear but ordinary differential equation if $\tilde{D}$ is a function of $C(x)$ alone. He introduced the variable

$$\eta \equiv \frac{x - x_M}{2\sqrt{t}} , \tag{10.2}$$

which is a combination of the space and time variables x and t, respectively. x_M refers to a special reference plane – the so-called *Matano plane* – to be defined below. Applying chain-rule differentiation to Eq. (10.1), we get the following identity:

$$\frac{\partial}{\partial x} \equiv \frac{\mathrm{d}}{\mathrm{d}\eta}\frac{\partial \eta}{\partial x} = \frac{1}{2\sqrt{t}}\frac{\mathrm{d}}{\mathrm{d}\eta} . \tag{10.3}$$

The operator on the left-hand side of Eq. (10.1) is

$$\frac{\partial}{\partial t} \equiv \frac{\mathrm{d}}{\mathrm{d}\eta}\frac{\partial \eta}{\partial t} = -\frac{x - x_M}{4t^{3/2}}\frac{\mathrm{d}}{\mathrm{d}\eta} = -\frac{\eta}{2t}\frac{\mathrm{d}}{\mathrm{d}\eta} . \tag{10.4}$$

The right-hand side of Eq. (10.1) can also be written in terms of η as

$$\frac{\partial}{\partial x}\left[\tilde{D}(C)\frac{\partial C}{\partial x}\right] = \frac{\mathrm{d}}{\mathrm{d}\eta}\frac{\partial \eta}{\partial x}\left[\frac{\tilde{D}(C)}{2\sqrt{t}}\frac{\mathrm{d}C}{\mathrm{d}\eta}\right] = \frac{1}{4t}\frac{\mathrm{d}}{\mathrm{d}\eta}\left[\tilde{D}(C)\frac{\mathrm{d}C}{\mathrm{d}\eta}\right] . \tag{10.5}$$

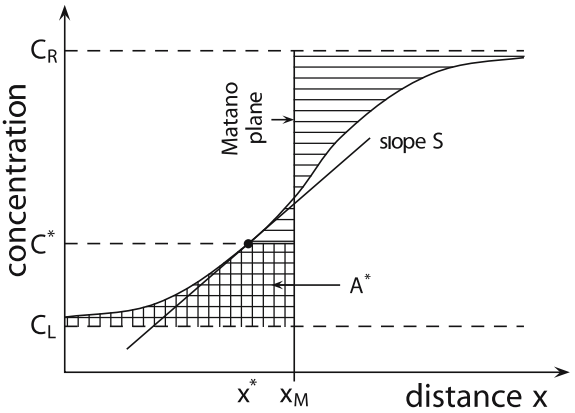

Fig. 10.1. Schematic illustration of the Boltzmann-Matano method for a binary diffusion couple with starting compositions C_L and C_R

By recombining left- and right-hand sides and using the Boltzmann variable we get Fick's second law as an ordinary differential equation for $C(\eta)$:

$$-2\eta\frac{\mathrm{d}C}{\mathrm{d}\eta} = \frac{\mathrm{d}}{\mathrm{d}\eta}\left[\tilde{D}(C)\frac{\mathrm{d}C}{\mathrm{d}\eta}\right] . \tag{10.6}$$

Some authors omit the factor 2 in the definition Eq. (10.2) of η. Then, a factor of 1/2 instead of 2 appears in the equation corresponding to Eq. (10.6). However, when finally transformed in ordinary time and space coordinates, the solutions obtained are identical.

10.1.2 Boltzmann-Matano Method

The Boltzmann-transformed version of Fick's second law Eq. (10.6) is a nonlinear ordinary differential equation. This equation allows us to deduce the concentration-dependent interdiffusion coefficient from an experimental concentration-depth profile, $C(x)$. Appropriate boundary conditions for an interdiffusion experiment have been suggested by the Japanese scientist Matano in 1933 [2]. He considered a binary diffusion couple, which consists of two semi-infinite bars joined at time $t = 0$. The initial conditions are

$$\begin{aligned} C &= C_L \quad \text{for} \quad (x < 0,\, t = 0), \\ C &= C_R \quad \text{for} \quad (x > 0,\, t = 0)\,. \end{aligned} \tag{10.7}$$

During a diffusion anneal of time t, a concentration profile $C(x)$ develops. This profile can be measured on a cross section of the diffusion zone, e.g., by electron microprobe analysis (see Chap. 13). Such a profile is schematically illustrated in Fig. 10.1.

Carrying out an integration between C_L and a fixed concentration C^*, we get from Eq. (10.6)

$$-2\int_{C_L}^{C^*}\eta \mathrm{d}C = \tilde{D}\left(\frac{\mathrm{d}C}{\mathrm{d}\eta}\right)_{C^*} - \tilde{D}\left(\frac{\mathrm{d}C}{\mathrm{d}\eta}\right)_{C_L} . \tag{10.8}$$

Matano's geometry guarantees vanishing gradients $dC/d\eta$ as C^* approaches C_L (or C_R). Using $(dC/d\eta)_{C_L} = 0$ and solving Eq. (10.8) for $\tilde{D}$ yields

$$\tilde{D}(C^*) = -2\frac{\int_{C_L}^{C^*}\eta \mathrm{d}C}{(\mathrm{d}C/\mathrm{d}\eta)_{C=C^*}} . \tag{10.9}$$

We transform Eq. (10.9) back to space and time coordinates using the Boltzmann variable Eq. (10.2) and get

$$\tilde{D}(C^*) = -\frac{1}{2t}\frac{\int_{C_L}^{C^*}(x - x_M)\mathrm{d}C}{(\mathrm{d}C/\mathrm{d}x)_{C^*}} . \tag{10.10}$$

This relation is called the *Boltzmann-Matano equation*. It permits us to determine $\tilde{D}$ for any C^* from an experimental concentration-distance profile. For the analysis, the position of the *Matano plane*, x_M, must be known. Carrying out the integration between the limits C_L and C_R, we get from Eq. (10.6)

$$\int_{C_L}^{C_R}\eta \mathrm{d}C = 0 . \tag{10.11}$$

Equation (10.11) can be considered as the definition of the Matano plane. x_M must be chosen in such a way that Eq. (10.11) is fulfilled.

In order to determine the Matano plane, we have to remember that at the beginning of the experiment the concentration of the diffusing species was C_L (C_R) on the left-hand (right-hand) side. Let us suppose, for example, $C_L < C_R$. Then, at the end of the experiment, the surplus of the diffusing species found on the left-hand side must have arrived by diffusion from the right-hand side. The location of the Matano plane can be determined from the conservation condition

$$\underbrace{\int_{-\infty}^{x_M}[C(x) - C_L]\,\mathrm{d}x}_{gain} = \underbrace{\int_{x_M}^{\infty}[C_R - C(x)]\,\mathrm{d}x}_{loss} . \tag{10.12}$$

When integrated by parts, the integrals in Eq. (10.12) transform to integrals with C as the running variable instead of x. If we apply the Matano boundary conditions Eq. (10.7), we get

$$(C_L - C_R)x_M + \int_{C_L}^{C_M} x\mathrm{d}C + \int_{C_M}^{C_R} x\mathrm{d}C = 0 , \tag{10.13}$$

where C_M denotes the concentration at the Matano plane. If we choose the Matano plane as origin of the x-axis ($x_M = 0$), the first term in Eq. (10.13) vanishes. Then, the following integrals balance across the Matano plane:

$$\int_{C_R}^{C_M} x \mathrm{d}C + \int_{C_M}^{C_L} x \mathrm{d}C = 0\,. \tag{10.14}$$

Although the location of the Matano plane is not known a priori, it can be found from experimental concentration-distance data by balancing the horizontally hatched areas in Fig. 10.1.

In summary, the determination of interdiffusion coefficients from an experimental concentration-distance profile via the Boltzmann-Matano method requires the following steps:

1. Determine the position of the Matano plane from Eq. (10.11) and use this position as the origin of the x-axis.
2. Choose C^* and determine the integral $\int_{C_L}^{C^*} x \mathrm{d}C$ from the experimental concentration-distance data. The integral corresponds to the double-hatched area A^* in Fig. 10.1.
3. Determine the concentration gradient $S = (\mathrm{d}C/\mathrm{d}x)_{C^*}$. S corresponds to the slope of the concentration-distance curve at the position x^*.
4. Determine the interdiffusion coefficient $\tilde{D}$ for $C = C^*$ from the Boltzmann-Metano equation (10.10) as: $\tilde{D}(C^*) = -A^*/(2tS)$.

We draw the readers attention to the following points:

(i) The Boltzmann-Matano equation (10.10) refers to an 'infinite' system. Its application to an experiment requires that the concentration changes must not have reached the boundaries of the system.

(ii) Close to the end-member compositions, the Boltzmann-Matano procedure may incur relatively large errors in $\tilde{D}$ because far away from the Matano plane both the integral A^* and the slope S become very small.

(iii) The initial interface of a diffusion couple can be tagged by inert diffusion markers (e.g., ThO_2 particles, thin Mo or W wires). The plane of the markers in the diffusion couple is denoted as the *Kirkendall plane*. Usually, for $t \neq 0$ the positions of the Matano plane and of the Kirkendall plane will be different. This is called the *Kirkendall effect* and is discussed in Sect. 10.2.

(iv) This method is applicable when the volume of the diffusion couple does not change during interdiffusion.

The Boltzmann-Matano method has been modified by Sauer and Freise [3] and later by den Broeder [4]. These authors introduce a normalised concentration variable Y defined by:

$$Y = \frac{C - C_R}{C_L - C_R}\,. \tag{10.15}$$

If no volume change occurs upon interdiffusion, the Sauer-Freise solution can be written in the following way:

$$\tilde{D}(C^*) = \frac{1}{2t(\mathrm{d}C/\mathrm{d}x)_{x^*}} \left[(1-Y)) \int_{x^*}^{\infty} (C^* - C_R)\mathrm{d}x + Y \int_{-\infty}^{x^*} (C_L - C^*)\mathrm{d}x \right] . \tag{10.16}$$

Here C^* is the concentration at the position x^*. The Sauer-Freise approach circumvents the need to locate the Matano plane. In this way, errors associated with finding its position are eliminated. On the other hand, application of Eq. (10.16) to the analysis of an experimental interdiffusion profile, like the Boltzmann-Matano method, requires the computation of two integrals and of one slope.

10.1.3 Sauer-Freise Method

When the volume of a diffusion couple changes during interdiffusion neither the Boltzmann-Matano equation (10.10) nor Eq. (10.16) can be used. Fick's law then needs a correction term [5, 6]. Volume changes in a binary diffusion couple occur whenever the total molar volume V_m of an A-B alloy deviates from *Vegard's rule*, which states that the total molar volume of the alloy is obtained from $V_m = V_A N_A + V_B N_B$, where V_A, V_B denote the molar volumes of the pure components and N_A, N_B the molar fractions of A and B in the alloy. Vegard's rule is illustrated by the dashed line in Fig. 10.2.

Non-ideal solid solution alloys exhibit deviations from Vegard's rule, as indicated by the solid line in Fig. 10.2. Diffusion couples of such alloys change their volume during interdiffusion. Couples with positive deviations from Vegard's rule swell, couples with negative deviations shrink. The partial molar volumes of the components A and B, $\tilde{V}_A \equiv \partial V_m/\partial N_A$ and $\tilde{V}_B \equiv \partial V_m/\partial N_B$, are related to the total molar volume via:

$$V_m = \tilde{V}_A N_A + \tilde{V}_B N_B \,. \tag{10.17}$$

As indicated in Fig. 10.2, the partial molar volumes can be obtained graphically as intersections of the relevant tangent with the ordinate.

Sauer and Freise [3] deduced a solution for interdiffusion with volume changes. Instead of Eq. (10.15), they introduced the ratio of the mole fractions

$$Y = \frac{N_i - N_i^R}{N_i^L - N_i^R} \,, \tag{10.18}$$

with N_i^L and N_i^R being the unreacted mole fractions of component i at the left-hand or right-hand side of the diffusion couple. The interdiffusion coefficient $\tilde{D}$ is then obtained from

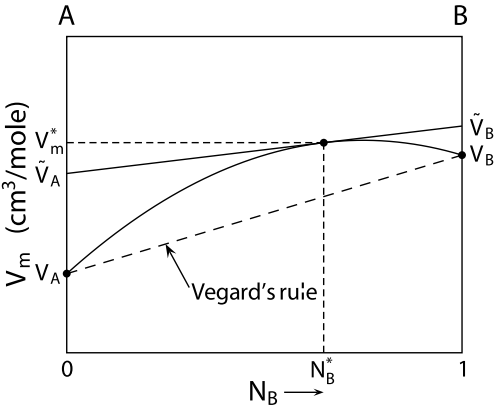

Fig. 10.2. Molar volume of an A-B solid solution alloy (*solid line*) *versus* composition. The *dashed line* repesents the *Vegard rule*. The partial molar volumes, $\tilde{V}_A$ and $\tilde{V}_B$, and the molar volumes of the pure components, V_A and V_B, are also indicated

$$\tilde{D}(Y^*) = \frac{V_m}{2t(dY/\mathrm{d}x)_{x^*}} \left[(1 - Y^*) \int_{-\infty}^{x^*} \frac{Y}{V_m} \mathrm{d}x + Y^* \int_{x^*}^{+\infty} \frac{1 - Y}{V_m} \mathrm{d}x \right] . \quad (10.19)$$

In order to evaluate Eq. (10.19), it is convenient to construct from the experimental composition-distance profile and from the V_m data two graphs, namely the integrands Y/V_m and $(1 - Y)/V_m$ *versus* x, as illustrated in Fig. 10.3. The two integrals in Eq. (10.19) correspond to the hatched areas. Equations (10.19) and (10.16) contain two infinite integrals in the running variable. Their application to the analysis of an experimental concentration-depth profile requires accurate computation of a gradient and of two integrals.

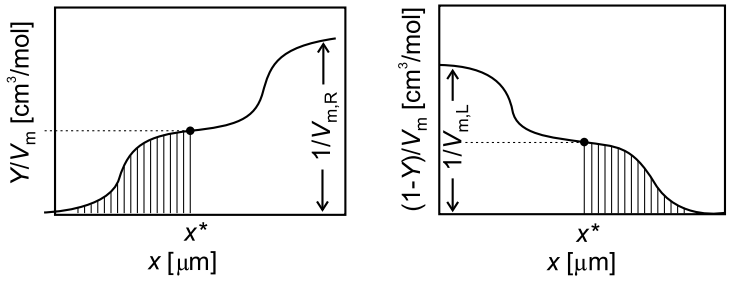

Fig. 10.3. Composition profiles constructed according to the Sauer-Freise method. $V_{m,L}$ and $V_{m,R}$ are the molar volumes of the left-hand and right-hand end-members of the diffusion couple

10.2 Intrinsic Diffusion and Kirkendall Effect

So far, we have described diffusion of a two-component system by a single interdiffusion coefficient, which depends on composition. In general, the rate of transfer of A atoms is greater/smaller than that of B atoms. Thus, there are two diffusion coefficients, D_A^I and D_B^I, which are denoted as the *intrinsic diffusion coefficients* of the components. They are concentration dependent as well. On the other hand, there is only one diffusion process, namely the intermixing of A and B. These two apparently contradictory facts are closely related to the question of how we specify the reference frame for the diffusion process. We know that the atoms in a crystalline solid are held in a lattice structure and we shall therefore retain the form of Fick's first law for the diffusion fluxes relative to a frame fixed in the local crystal lattice (intrinsic diffusion fluxes):

$$j_A = -D_A^I \frac{\partial C_A}{\partial x}, \quad j_B = -D_B^I \frac{\partial C_B}{\partial x}\,. \tag{10.20}$$

The inequality of these fluxes leads to a net mass flow accompanying the interdiffusion process, which causes the diffusion couple to shrink on one side and to swell on the other side. This observation is called the *Kirkendall effect*. It was discovered by KIRKENDALL AND COWORKERS in a copper-brass diffusion couple in the 1940s [7, 8]. The Kirkendall shift can be observed by incorporating inert inclusions, called markers (e.g., Mo or W wires, ThO_2 particles), at the interface where the diffusion couple is initially joined. The original Kirkendall experiment is illustrated in Fig. 10.4. It showed that Zn atoms diffused faster outwards than Cu atoms inward ($D_{Zn}^I > D_{Cu}^I$) causing the inner brass core to shrink. This in turn resulted in the movement of the inert Mo wires. In the period since, it has been demonstrated that the Kirkendall effect is a widespread phenomenon of interdiffusion in substitutional alloys.

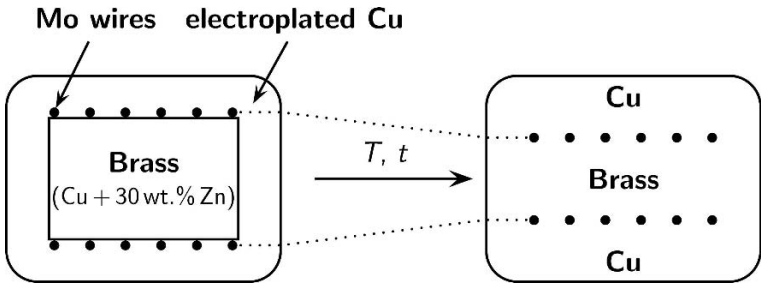

Fig. 10.4. Schematic illustration of a cross section of a diffusion couple composed of pure Cu and brass (Cu-Zn) prepared by SMIGELSKAS AND KIRKENDALL [8] before and after heat treatment. The Mo markers placed at the original contact surface moved towards each other. It was concluded that Zn atoms diffused faster outwards than Cu atoms move inwards ($D_{Zn}^I > D_{Cu}^I$)

The Kirkendall effect was received by contemporary scientists with much surprise. Before the 1940s it was commonly believed that diffusion in solids takes place via direct exchange or ring mechanism (see Chap. 6), which imply that the diffusivities of both components of a binary alloy are equal. The fact that in a solid-state diffusion process the species diffuse at different rates changed the existing atomistic models on solid-state diffusion completely. The Kirkendall effect lended much support to the vacancy mechanism of diffusion[1].

The position of the Kirkendall plane, x_K, moves parabolically in time with respect to the laboratory-fixed frame:

$$x_K = K\sqrt{t}\,. \tag{10.21}$$

Here K is a (temperature-dependent) constant. The parabolic shift indicates that we are dealing with a diffusion-controlled process. We also note that the Kirkendall plane is the only marker plane that starts moving from the beginning. The *Kirkendall velocity* v_K is given by

$$v_K \;\equiv\; \frac{dx_K}{\mathrm{d}t} = \frac{x_K}{2t} \tag{10.22}$$

From the position of the Kirkendall plane one can deduce information about the intrinsic diffusivities. Van Loo showed that their ratio is given by [10]:

$$\frac{D_A^I}{D_B^I} = \frac{\tilde{V}_A}{\tilde{V}_B}\left[\frac{N_A^R \int_{-\infty}^{x_K} \frac{1}{V_m}(N_A - N_A^L)\mathrm{d}x - N_A^L \int_{x_K}^{\infty} \frac{1}{V_m}(N_A^R - N_A)\mathrm{d}x}{-(N_B^R) \int_{-\infty}^{x_K} \frac{1}{V_m}(N_A - N_A^L)\mathrm{d}x + N_B^L \int_{x_K}^{\infty} \frac{1}{V_m}(N_A^R - N_A)\mathrm{d}x}\right]. \tag{10.23}$$

N_i is the mole fraction of component i, with N_i^L and N_i^R the unreacted left-hand ($x \to -\infty$) and right-hand ($x \to -\infty$) ends of the couple, respectively.

Since the discovery of the Kirkendall effect by Smigelskas and Kirkendall [8] and its analysis by Darken [9], this effect assumed a prominent rôle in the diffusion theory of metals. It was considered as evidence for vacancy-mediated diffusion in solids. There are also technological fields in which the Kirkendall effect is of great interest. Examples are composite materials, coating technologies, microelectronic devices, etc. The interactions accompanying the Kirkendall effect between constituents of such structures can, for example, induce stress and even deformation on a macroscopic scale. It can also cause migration of microscopic inclusions inside a reaction zone and Kirkendall porosity.

[1] Nowadays, we know that the Kirkendall effect can manifest itself in many phenomena such as the development of diffusional porosity (Kirkendall voids), generation of internal stresses [13, 14], and even by deformation of the material on a macroscopic scale [15]. These diffusion-induced processes are of concern in a wide variety of structures including composite materials, coatings, welded components, and thin-film electronic devices.

10.3 Darken Equations

The first theoretical desciption of interdiffusion and Kirkendall effect was attempted by Darken in 1948 [9]. For a binary substitutional alloy he used the two intrinsic diffusivities introduced above to describe the interdiffusion process. The Kirkendall velocity v_K can be expressed in terms of the intrinsic fluxes, j_A and j_B, and partial molar volumes, $\tilde{V}_A$ and $\tilde{V}_B$, as

$$v_K = -(\tilde{V}_A j_A + \tilde{V}_B j_B)\,. \tag{10.24}$$

Given the fact that $\mathrm{d}C_A = -(\tilde{V}_B/\tilde{V}_A)\mathrm{d}C_B$, we can write for the Kirkendall velocity

$$v_K = \tilde{V}_B(D_B^I - D_A^I)\frac{\partial C_B}{\partial x}\,, \tag{10.25}$$

where $\partial C_B/\partial x$ denotes the concentration gradient at the Kirkendall plane. Following Darken's approach, the laboratory-fixed interdiffusion flux J (at the Kirkendall plane) can be written as the sum of an intrinsic diffusion flux of one of the components i plus (or minus) a Kirkendall drift term $v_K C_i$:

$$J = -D_i^I \frac{\partial C_i}{\partial x} \;\pm v_K C_i \quad i = A, B\,. \tag{10.26}$$

Substituting Eq. (10.25) in Eq. (10.26) one arrives at a general expression for the interdiffusion coefficient:

$$\tilde{D} = C_B \tilde{V}_B D_A^I + C_A \tilde{V}_A D_B^I\,. \tag{10.27}$$

Equations (10.25) and (10.27) provide a description of isothermal diffusion in a binary substitutional alloy. They also provide a possibility to determine the intrinsic diffusivities from measurements of the interdiffusion coefficient and the Kirkendall velocity.

From a fundamental point of view, the assumption that the concentration gradients are the driving forces of diffusion as given by Fick's laws is not correct. Instead, as already stated at the beginning of this chapter, the gradient of the chemical potential μ_i of component i is the real driving force. The flux of component i ($i = A, B$) in a binary alloy can be written as [16, 17]

$$j_i = -B_i C_i \frac{\partial \mu_i}{\partial x}\,, \tag{10.28}$$

where B_i denotes the mobility of component i. The chemical potential can be expressed in terms of the thermodynamic activity, a_i, via

$$\mu_i = \mu_i^0 + RT \ln a_i\,, \tag{10.29}$$

where μ_i^0 is the standard chemical potential (at 298 K and 1 bar) and R is the ideal gas constant ($R = 8.3143$ J mol^{-1}K^{-1}). The atomic mobility B_i

is connected to the tracer diffusion coefficient D_i^* of component i via the Nernst-Einstein relation (see Chap. 11):

$$D_i^* = B_i RT\,. \tag{10.30}$$

Substituting Eqs. (10.30) and (10.28) in Eq. (10.20) and knowing that $C_A = N_A/V_m$ and $\mathrm{d}N_A = (V_m^2/\tilde{V}_A)\mathrm{d}C_A$ one obtains relations between the intrinsic and the tracer diffusion coefficients:

$$D_A^I = D_A^* \frac{V_m}{\tilde{V}_B} \frac{\partial \ln a_A}{\partial \ln N_A} \quad \text{and} \quad D_B^I = D_B^* \frac{V_m}{\tilde{V}_A} \frac{\partial \ln a_B}{\partial \ln N_B}\,. \tag{10.31}$$

The quantity $\Phi \equiv \partial \ln a_i / \partial \ln N_i$ is denoted as the *thermodynamic factor*.

The thermodynamics of binary systems tells us that the thermodynamic factor can also be expressed as follows [21]:

$$\Phi = \frac{N_A\, N_B}{RT} \frac{\mathrm{d}^2 G}{\mathrm{d}N_i^2} = \frac{\partial \ln a_i}{\partial \ln N_i} = 1 + \frac{\partial \ln \gamma_i}{\partial \ln N_i}\,, \tag{10.32}$$

Here G denotes the Gibbs free energy and $\gamma_i \equiv a_i/N_i$ the coefficient of thermodynamic activity of species i (= A or B). In addition, as a consequence of the Gibbs-Duhem relation there is only one thermodynamic factor for a binary alloy:

$$\Phi = \frac{\partial \ln a_A}{\partial \ln N_A} = \frac{\partial \ln a_B}{\partial \ln N_B} \tag{10.33}$$

Substiting Eq. (10.31) in Eq. (10.27) and knowing the relation $C_i \equiv N_i(C_A + C_B) = N_i/V_m$ between concentrations and mole fractions, we obtain for the interdiffusion coefficient

$$\tilde{D}_{Darken} = (N_A D_B^* + N_B D_A^*)\, \Phi\,. \tag{10.34}$$

Equations (10.31) and (10.34) are called the *Darken equations*. Sometimes the name *Darken-Dehlinger equations* is used. These relations are widely used in practice for substitutional binary alloys. Their simplicity provides an obvious convenience. We shall assess its accuracy below and also in Chap. 12.

If thermodynamic data are available, either from activity measurements or from theoretical models, Eqs. (10.31) or (10.34) allow to relate the intrinsic diffusivities and the interdiffusion coefficient to the tracer diffusivities. For an ideal solid solution alloy we have $\gamma_i = 1$ and $a_i = N_i$ and hence $\Phi = 1$ (Raoult's law). For non-ideal solutions Φ deviates from unity. It is larger than unity for phases with negative deviations of G from ideality and smaller than unity in the opposite case. Negative deviations are expected for systems with order. Therefore, thermodynamic factors of intermetallic compounds are often larger, sometimes even considerably larger than unity due to the attractive interaction between the constituents of the intermetallic phase. As a consequence, interdiffusion coefficients are often larger than the term in paranthesis of Eq. (10.34).

10.4 Darken-Manning Equations

Soon after the detection of the Kirkendall effect and its phenomenological description via the Darken equations, Seitz in 1948 [11] and Bardeen in 1949 [12] recognised that the original Darken equations are approximations. From an atomistic point of view, interdiffusion in substitutional alloys is mediated by vacancies. It was shown that the Darken equations are obtained if the concentration of vacancies is in thermal equilibrium during the interdiffusion process. For the Kirkendall effect to occur, vacancies must be created at one site and annihilated on the other side of the interdiffusion zone so that a vacancy flux is created to maintain local equilibrium. This implies that sources and sinks for vacancies are abundant in the diffusion couple. The vacancy flux causes the so-called vacancy-wind effect – a correction term that must be added to the original Darken equations to obtain the Darken-Manning relations.

The relations between tracer diffusivities and intrinsic diffusivities and the interdiffusion coefficient discussed in the previous section are incomplete for a vacancy mechanism, because of correlation effects. The exact expressions are similar to those discussed above but with *vacancy-wind factors* (see, e.g., [17, 21, 22]). The intrinsic diffusion coefficients Eq. (10.31) with vacancy-wind corrections, r_A and r_B, can be written as

$$D_A^I = D_A^* \frac{V_m}{\tilde{V}_B} \Phi r_A \quad \text{and} \quad D_B^I = D_B^* \frac{V_m}{\tilde{V}_A} \Phi r_B \,. \tag{10.35}$$

The vacancy-wind factors can be expressed in terms of the tracer and collective correlation factors:

$$r_A = \frac{f_{AA} - N_A f_{AB}^{(A)}/N_B}{f_A} \quad \text{and} \quad r_B = \frac{f_{BB} - N_A f_{AB}^{(B)}/N_A}{f_A} \,. \tag{10.36}$$

The f_i are the tracer correlation factors and f_{ij} the collective correlation factors sometimes also called correlations functions [22] (see also Chap. 12).

Perhaps the best-known vacancy-wind factor is the total vacancy-wind factor, S, occuring in the generalised Darken equation:

$$\tilde{D} = (N_A D_B^* + N_B D_A^*)\, \Phi S = \tilde{D}_{Darken} S \,. \tag{10.37}$$

Equation (10.37) is also called the *Darken-Manning equation* and S is also denoted as the *Manning factor*. It can be expressed as

$$S = \frac{N_A D_B^* r_B + N_B D_A^* r_A}{N_A D_B^* + N_B D_A^*} \,. \tag{10.38}$$

Manning [18, 19] developed approximate expressions for vacancy-wind factors in the framework of a model called the *random alloy model*. The term random alloy implies that vacancies and A and B atoms are distributed at

random on the same lattice, although the rates at which atoms exchange with vacancies are allowed to be different. For a random alloy, the individual vacancy-wind factors are

$$r_A = 1 + \frac{(1-f)}{f}\frac{N_A(D_A^* - D_B^*)}{(N_A D_A^* + N_B D_B^*)} \quad \text{and}$$

$$r_B = 1 + \frac{(1-f)}{f}\frac{N_A(D_B^* - D_A^*)}{(N_A D_A^* + N_B D_B^*)}\,, \tag{10.39}$$

where f is the tracer correlation factor for self-diffusion. A transparent derivation of Eq. (10.39) can be found in [20]. For convenience let us assume that $D_A^* \geq D_B^*$. Then, from these expressions we see that the factors r_A and r_B take the limits

$$1.0 \leq r_A \leq \frac{1}{f} \quad \text{and} \quad 0.0 \leq r_B \leq 1.0\,. \tag{10.40}$$

There is also a 'forbidden region' $N_A \leq 1 - f$, where r_B can take negative values (unphysical for this model) if $D_A^*/D_B^* > N_B/(N_B - f)$. In other words, there is a concentration-dependent upper limit for the ratio of the tracer diffusivities in this region. Manning also provides an expression for the total vacancy-wind factor:

$$S = 1 + \frac{(1-f)}{f}\frac{N_A N_B (D_A^* - D_B^*)^2}{(N_A D_A^* + N_B D_B^*)(N_A D_B^* + N_B D_A^*)}\,. \tag{10.41}$$

From Eq. (10.41) it is seen that S varies within narrow limits:

$$1 \;\leq\; S \;\leq 1/f\,. \tag{10.42}$$

Thus, in the framework of the random alloy model the total vacancy-wind factor S is not much different from unity. The Manning expressions for the vacancy-wind factors have been used for some 30 years. Extensive computer simulations studies in simple cubic, fcc, and bcc random alloys by Belova and Murch [23] have shown that the Manning formalism is not as accurate as commonly thought. It is, however, a reasonable approximation when the ratio of the atom vacancy exchange rates are not too far from unity.

Vacancy-wind corrections for chemical diffusion in intermetallic compounds depend on the structure, the type of disorder and on the diffusion mechanism. Belova and Murch have also contributed significantly to chemical diffusion in ordered alloys by considering among others $L1_2$ structured compounds [24], $D0_3$ and A15 structured alloys [26], and B2 structured compounds [25].

10.5 Microstructural Stability of the Kirkendall Plane

Kirkendall effect induced migration of inert markers inside the diffusion zone and the uniqueness of the Kirkendall plane have not been questioned for

quite a long time. In recent years, the elucidation of the Kirkendall effect accompanying interdiffusion has taken an additional direction. Cornet and Calais [29] were the first to describe hypothetical diffusion couples in which more than one 'Kirkendall marker plane' can emerge. Experimental discoveries also revealed a more complex behaviour of inert markers situated at the original interface of a diffusion couple in both spatial and temporal domains. Systematic studies of the microstructural stability of the Kirkendall plane were undertaken by van Loo and coworkers [30–35]. Clear evidence for the ideas of Cornet and Calais was found and led to further developments in the understanding of the Kirkendall effect. In particular, it was found that the Kirkendall plane, under predictable circumstances, can be multiple, stable, or unstable.

The diffusion process in a binary A-B alloy can best be visualised by considering the intrinsic fluxes, j_A and j_B, of the components in Eq. (10.20) with respect to an array of inert markers positioned prior to annealing along the anticipated diffusion zone. According to Eq. (10.25) the sum of the oppositely directed fluxes of the components is equal to the velocity of the inert markers, v, with respect to the laboratory-fixed frame of reference:

$$v = \tilde{V}_B(D_B^I - D_A^I)\frac{\partial C_B}{\partial x}\,, \tag{10.43}$$

with $\tilde{V}_B$ being the partial molar volume of component B. Multifoil experiments, in which a diffusion couple is composed of many thin foils with markers at each interface, permit a determination of v at many positions inside a diffusion couple. Thus a v *versus* x curve (marker-velocity curve) can be determined experimentally.

In a diffusion-controlled intermixing process, those inert markers placed at the interface where the concentration step is located in the diffusion couple is the *Kirkendall plane*. The markers in the Kirkendall plane are the only ones that stay at a constant composition and move parabolically with a velocity given by Eq. (10.22), which we repeat for convenience:

$$v_K = \frac{\mathrm{d}x}{\mathrm{d}t} = \frac{x_K}{2t}\,. \tag{10.44}$$

x_K is the position of the Kirkendall plane at time t.

The location of the Kirkendall plane(s) in the diffusion zone can be found graphically at the point(s) of intersection(s) between the marker-velocity curve and the straight line given by Eq. (10.44) (see Fig. 10.5). In order to draw the line $v_K = x_K/2t$, one needs to know the position in the diffusion zone where the 'Kirkendall markers' were located at time $t = 0$. If the total volume does not change during interdiffusion this position can be determined via the usual Boltzmann-Matano analysis. If the partial molar volumes are composition dependent, the Sauer-Freise method should be used.

The nature of the Kirkendall plane(s) in a diffusion couple depends on the gradient of the marker-velocity curve at the point of intersection with the

straight line $x_K/2t$. For illustration, let us consider a hypothetical diffusion couple of A-B alloys with the end-members A_yB_{1-y} and A_zB_{1-z} where $y > z$. Let us suppose that on the A-rich side of the diffusion zone A is the faster diffusing species, whereas on the B-rich side B is the faster diffusing species. Figure 10.5 shows schematic representations of the marker-velocity curves in different situations. For some diffusion couples the straight line, $v_K = x/2t$, may intersect the marker-velocity curve in the diffusion zone once at a point with a negative gradient (upper part). At this point of intersection one can expect *one stable Kirkendall plane*. Markers, which by some perturbation

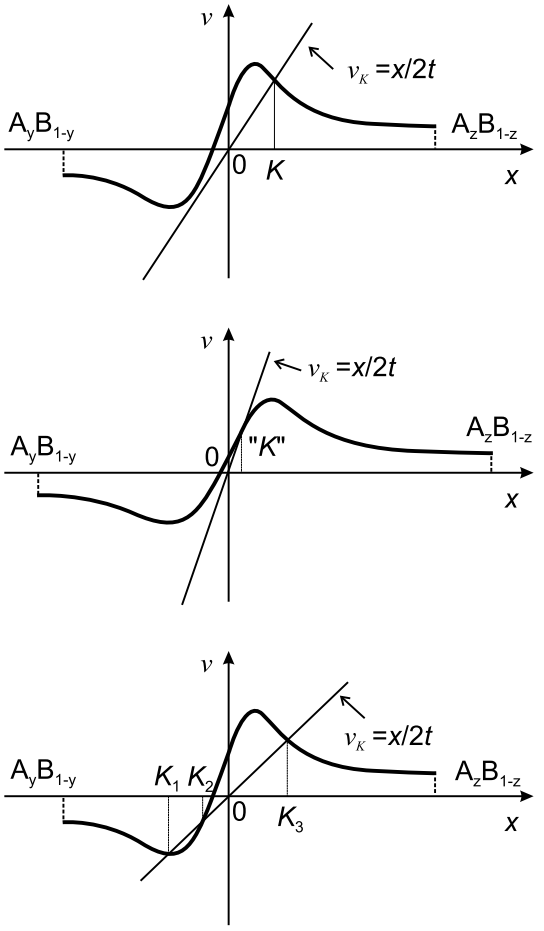

Fig. 10.5. Schematic velocity diagrams, pertaining to diffusion couples between the end-members A_yB_{1-y} and A_zB_{1-z} for $y > z$. On the A-rich side A diffuses faster and on the B-rich side B diffuses faster. Different situations are shown, which pertain to one stable Kirkendall plane (*upper part*), to an unstable plane (*middle part*), and to two stable Kirkendall planes, K_1 and K_3, and an unstable plane K_2

move ahead of the Kirkendall plane, will slow down, because of the lower velocity; markers behind this plane will move faster. The stable Kirkendall plane acts as an 'attractor for inert markers'. By changing the end-member compositions the straight line, $v_K = x/2t$, may intersect the marker-velocity curve at a point with a positive velocity gradient (middle part). Markers slightly ahead of this plan will move faster, whereas markers behind this plane will move slower. This will result in scatter of the markers and there will be no unique plane acting as the Kirkendall plane (*unstable Kirkendall plane*). The lower part of Fig. 10.5 illustrates a situation where the straight line intersects the marker-velocity curve three times at K_1, K_2, and K_3. In this case one might expect that three Kirkendall planes will be present in the sample. In reality, one finds *two stable Kirkendall planes*, K_1 and K_3. An unstable plane, K_2, is located between two stable Kirkendall planes and the stable planes will accumulate the markers during the initial stage of interdiffusion.

The presence of stable and unstable Kirkendall planes has been verified, for example, in Ni-Pd and Fe-Pd diffusion couples [31]. The marker-velocity curves over the whole homogeneity range have been determined in multifoil experiments. It was indeed found that for Ni-Pd a stable Kirkendall plane is present and the straight line, $v_K = x/2t$, intersects the marker-velocity curve at a point with a negative gradient. An unstable Kirkendall plane is found in Fe-Pd and the gradient of the marker-velocity curve is positive at the intersection point.

References

1. L. Boltzmann, Wiedemanns Ann. Phys. **53** (1894) 959
2. C. Matano, Japan. J. Phys. **8** (1933) 109
3. F. Sauer and V. Freise, Z. Elektrochem. **66** (1962) 353
4. F.J.A. den Broeder, Scr. Metall. **3** (1969) 321
5. K. Wagner, Acta Metall. **17** (1969) 99
6. F.F.J. van Loo, Acta Metall. **18** (1970) 1107
7. E.O. Kirkendall, Trans. AIME **147**, 104 (1942)
8. A.D. Smigelskas, E.O. Kirkendall, Trans. AIME **171**, 130 (1947)
9. L.S. Darken, Transactions AIME **175**, 184 (1948)
10. F.J.J. van Loo, Progr. Solid State Chemistry **20**, 47 (1990)
11. F. Seitz, Phys. Rev. **74**, 1513 (1948)
12. J. Bardeen, Phys. Rev. **76**, 1403 (1949)
13. G.B. Stephenson, Acta Metall. **36**, 2663 (1988)
14. D.L. Beke, I.A. Szabo (Eds.), Proc. of Int. Workshop on *Diffusion and Stresses*, Balatonfüred, Hungary, May 1995; also: Defect and Diffusion Forum **129–130** (1996)
15. I. Daruka, I.A. Szabo, D.L. Beke, C. Cerhati, A.A. Kodentsov, F.J.J. van Loo, Acta Mater. **44**, 4981 (1996)
16. S. Prager, J. Chem. Phys. **21** 1344–1347 (1953)

17. A.R. Allnatt, A.B. Lidiard, *Atomic Transport in Solids*, Cambridge Univerity Press, 1993
18. J.R. Manning, *Diffusion Kinetics for Atoms in Crystals*, van Norstrand, Princeton, 1968
19. J.R. Manning, Acta Metall. **15**, 817 (1967)
20. R.E. Howard, A.B. Lidiard, *Matter Transport in Solids*, in: Reports on Progress in Physics, Vol. XXVII, The Institute of Physics and the Physical Society, London, 1964, pp. 161–240
21. J. Philibert, *Atom Movements – Diffusion and Mass Transport in Solids*, Les Editions de Physique, Les Ulis, 1991
22. G.E. Murch, Z. Qin, Defect and Diffusion Forum **109**, 1 (1994)
23. I.V. Belova, G.E. Murch, Philos. Mag. **A 80**, 1469–1479 (2000); Philos. Mag. **A 81**, 1749–1758 (2001)
24. I.V. Belova, G.E. Murch, Philos. Mag, **A 78**, 1085–1092 (1998)
25. I.V. Belova, G.E. Murch, Philos. Mag, **A 79**, 193–202 (1999)
26. I.V. Belova, G.E. Murch, J. Phys. Chem. Sol. **60**, 2023–2029 (1998)
27. I.V. Belova, G.E. Murch, Philos. Mag, **A 81**, 83–94 (2001)
28. I.V. Belova, G.E. Murch, Defect and Diffusion Forum **194–199**, 533–540 (2001)
29. J.-F. Cornet, D. Calais, J. Phys. Chem. Sol. **33**, 1675 (1972)
30. F.J.J. van Loo, B. Pieragi, R.A. Rapp, Acta Metall. Mater. **38**, 1769 (1990)
31. M.J.H. van Dal, M.C.I.P. Pleumeckers, A. A. Kodentsov, F.J.J. van Loo, Acta Mater. **48**, 385 (2000)
32. M.J.H. van Dal, A.M. Gusak, C. Cerhati, A. A. Kodentsov, F.J.J. van Loo, Phys. Rev. Lett. **86**, 3352 (2001)
33. M.J.H. van Dal, A.M. Gusak, C. Cerhati, A. A. Kodentsov, F.J.J. van Loo, Philos. Mag. A **82**, 943 (2002)
34. A. Paul, M.J.H. van Dal, A. A. Kodentsov, F.J.J. van Loo, Acta Mater. **52**, 623 (2004)
35. A. Paul, A.A. Kodentsov, F.J.J. van Loo, Defect and Diffusion Forum **237–240**, 813 (2005)